Supplement of Atmos. Chem. Phys., 20, 995–1020, 2020
https://doi.org/10.5194/acp-20-995-2020-supplement

Atmospheric Chemistry and Physics
Open Access

Supplement of

Using CESM-RESFire to understand climate–fire–ecosystem interactions and the implications for decadal climate variability

Yufei Zou et al.

Correspondence to: Yuhang Wang (yuhang.wang@eas.gatech.edu) and Yufei Zou (yufei.zou@pnnl.gov)

Supplement

Equation S1-S2

Figure S1-S6

Table S1

The AERONET network does not provide AOT measurements at 550 nm wavelength. For direct comparison with the model results, we estimated AERONET AOT at 550 nm by interpolating the measurements at two closest wavelengths at 500 nm and 675 nm. Specifically, the optical thickness of aerosols and the wavelength of light satisfies the power law (Ångström, 1929) in Eq. (S1):

$$\frac{\tau_\lambda}{\tau_{\lambda_0}} = \left(\frac{\lambda}{\lambda_0}\right)^{-\alpha}, \qquad \text{(S1)}$$

where τ_λ is the optical thickness at wavelength λ, τ_{λ_0} is the optical thickness at the reference wavelength λ_0, and α is the Ångström exponent.

We first calculated the Ångström exponent based on the optical thickness measured at 500 nm and 675 nm, then estimated the optical thickness at 550 nm using Eq. (S1) and AOT at 500 nm as the reference. The estimation equation is shown in Eq. (S2):

$$\tau_{550} = \tau_{500}\left(\frac{550}{500}\right)^{-\alpha},\ where\ \alpha = -\frac{log\frac{\tau_{675}}{\tau_{500}}}{\log\frac{675}{500}}\ . \text{(S2)}$$

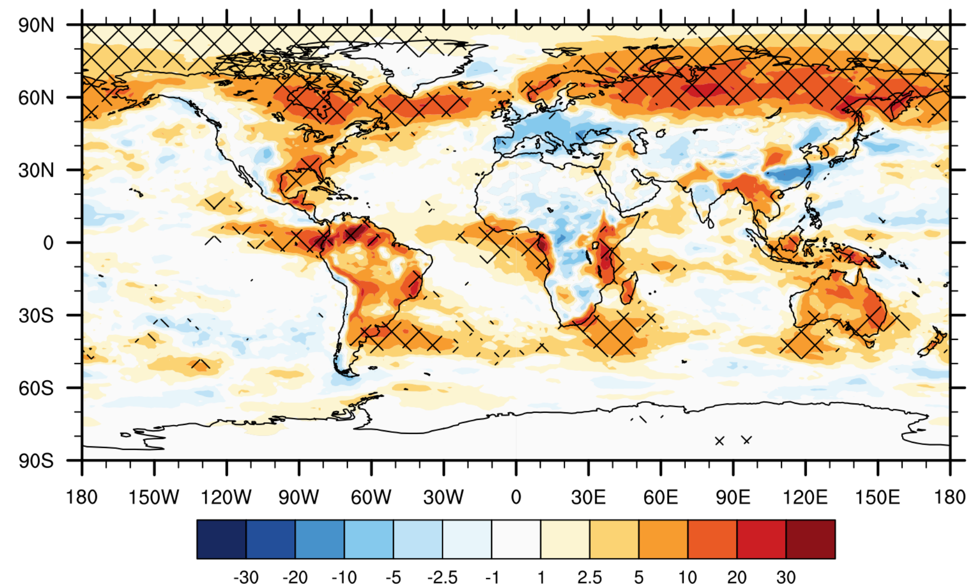

Figure S1: Fire aerosol-induced changes in low-level cloud fractions (unit: %) in the present-day simulation (CTRL1–SENS1A). The hatching denotes the 0.05 significance level.

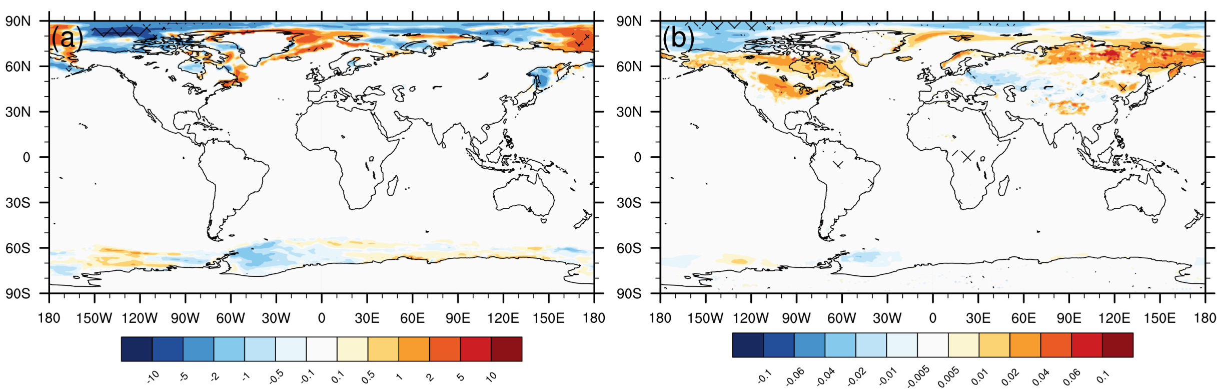

Figure S2: Fire aerosol-induced snow depth and surface albedo changes between CTRL1 and SENS1A (CTRL1–SENS1A). (a) changes in snow depths over ice (unit: m); (b) changes in surface albedo (unitless). The hatching denotes the 0.05 significance level.

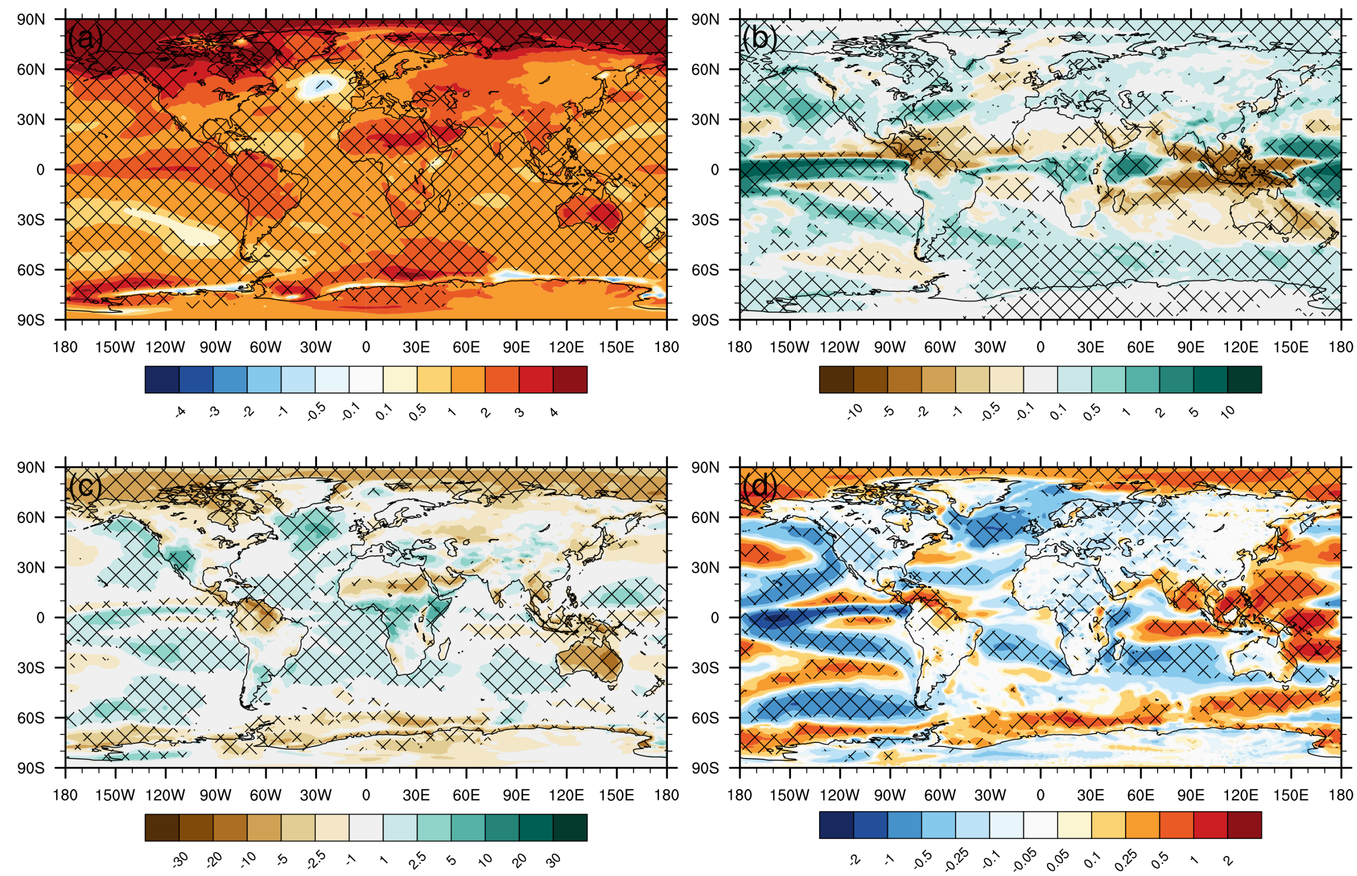

Figure S3: CESM-RESFire-simulated changes in fire weather variables without fire feedback between the RCP4.5 future scenario and the present-day scenario (SESN2B–SENS1B). (a) changes in surface temperature (unit: K); (b) changes in total precipitation rate (unit: mm day^{-1}); (c) changes in surface relative humidity (unit: %); (d) changes in surface wind speed (unit: m s^{-1}). The hatching denotes the 0.05 significance level.

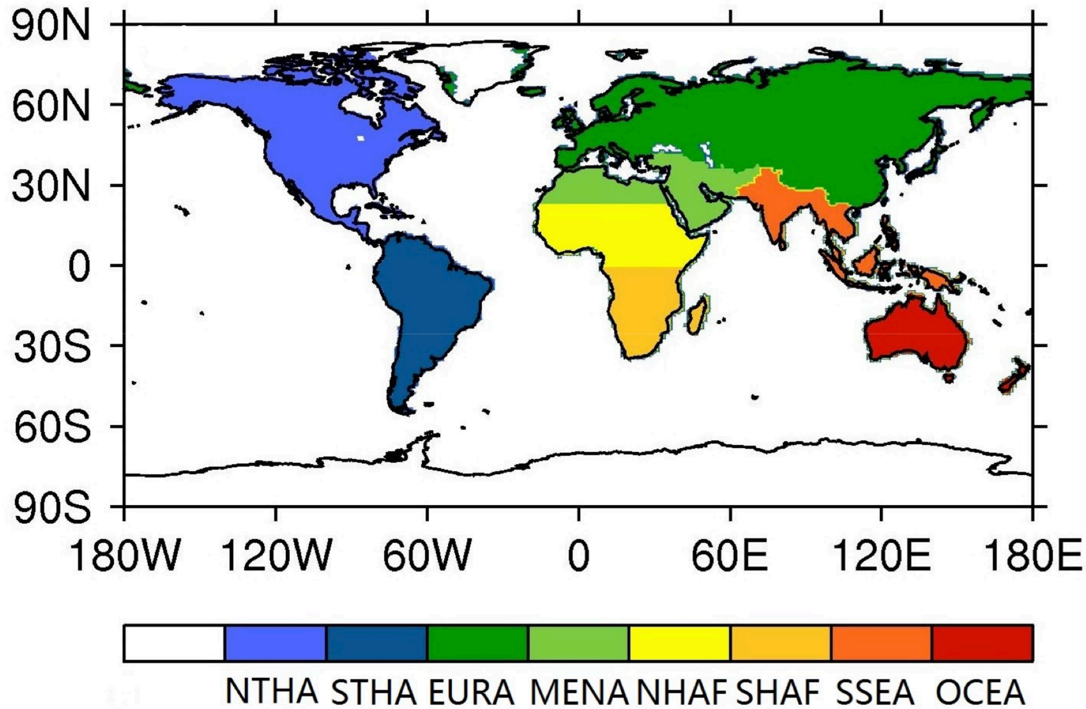

Figure S4: Geographical regions used for aggregating regional burned area in Fig. 11 of the manuscript. NTHA: North America; STHA: South America; EURA: Eurasia excluding Middle East and South Asia; MENA: Middle East and North Africa; NHAF: Northern Hemisphere Africa; SHAF: Southern Hemisphere Africa; SSEA: South and Southeast Asia; OCEA: Oceania.

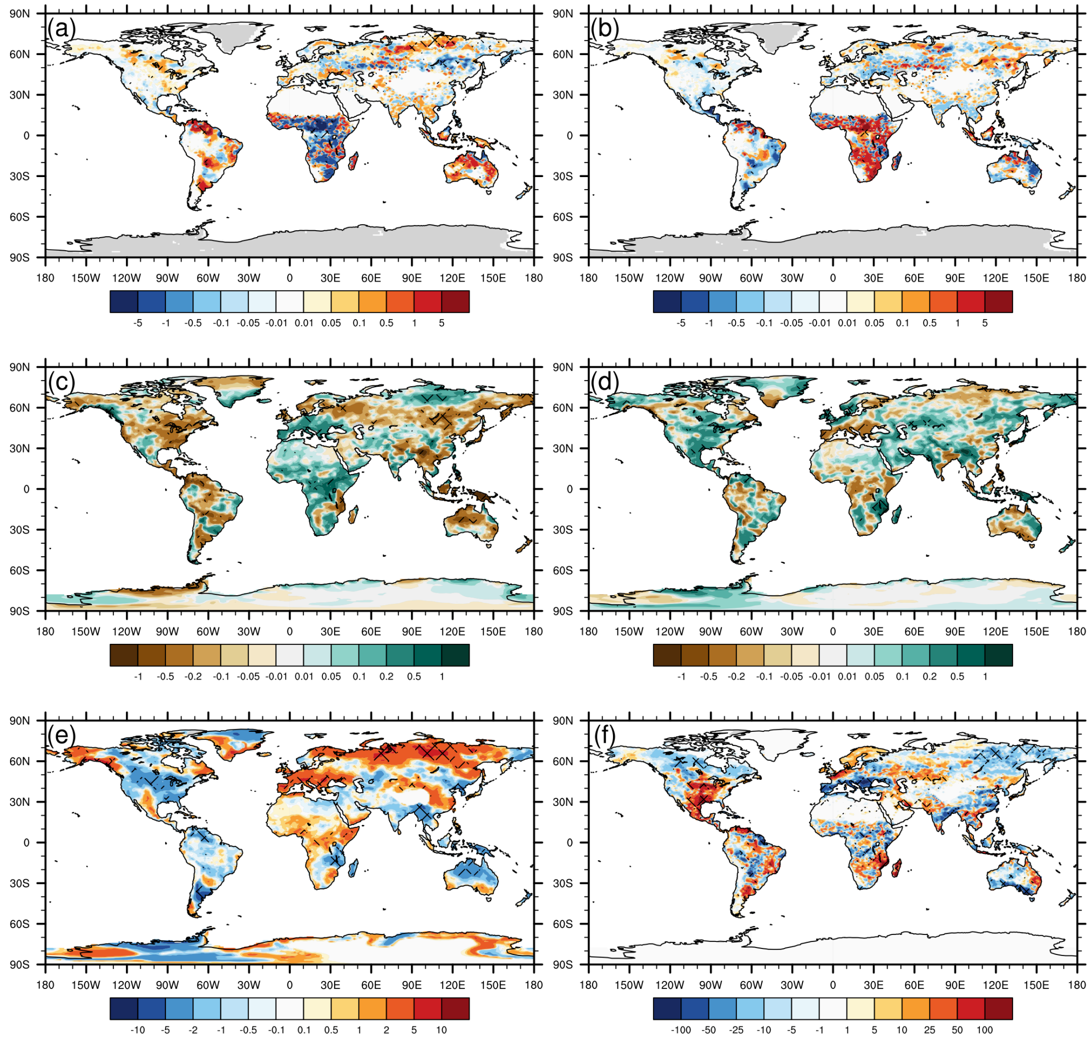

Figure S5: Comparison of two fire feedback pathways and associated atmospheric and vegetation processes. (a) changes in annual fractional burned area (unit: % yr^{-1}) induced by atmosphere-centric fire feedback ((CTRL2–CTRL1) – (SENS2A–SENS1A)); (b) changes in annual fractional burned area (unit: % yr^{-1}) induced by vegetation-centric fire feedback ((SENS2A–SENS1A) – (SENS2B–SENS1B)); (c) changes in precipitation rates (unit: mm day^{-1}) induced by atmosphere-centric fire feedback; (d) changes in precipitation rates (unit: mm day^{-1}) induced by vegetation-centric fire feedback; (e) changes in low level cloud fractions (unit: 100%) induced by atmosphere-centric fire feedback; (f) changes in vegetation evapotranspiration (unit: mm yr^{-1}) induced by vegetation-centric fire feedback. In (c), (d), and (e), only changes over land are shown for clear comparison with fire changes in (a) and (b). The hatching denotes the 0.05 significance level.

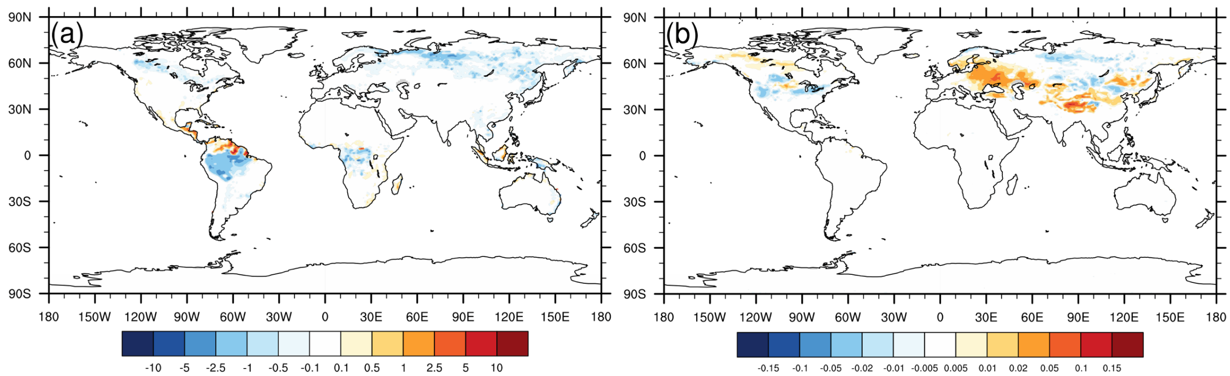

Figure S6: CESM-RESFire simulation of fire-related biophysical effects in the RCP4.5 future scenario. (a) differences of annual averaged fractional tree coverage (unit: %, SENS2A–SENS2B); (b) same as (a) but for differences of surface albedo (unitless) in early spring (January-April). The hatching denotes the 0.05 significance level.

Table S1: Assumed SOA (gas) yield in CAM5

Species	Mass yield	Reference
Big Alkanes	5%	Lim and Ziemann (2005)
Big Alkenes	5%	Assumed
Toluene	15%	Odum et al. (1997)
Isoprene	4%	Kroll et al. (2006)
Monoterpenes	25%	Ng et al. (2007)

References

Ångström, A.: On the Atmospheric Transmission of Sun Radiation and on Dust in the Air, Geografiska Annaler, 11, 2, 156–166. doi:10.1080/20014422.1929.11880498, 1929.

Kroll, J.H., Ng, N.L., Murphy, S.M., Flagan, R.C. and Seinfeld, J.H.: Secondary organic aerosol formation from isoprene photooxidation. Environmental science & technology, 40(6), 1869-1877, 2006.

Lim, Y.B. and Ziemann, P.J.: Products and mechanism of secondary organic aerosol formation from reactions of n-alkanes with OH radicals in the presence of NO x. Environmental science & technology, 39(23), 9229-9236, 2005.

Ng, N.L., Chhabra, P.S., Chan, A.W.H., Surratt, J.D., Kroll, J.H., Kwan, A.J., McCabe, D.C., Wennberg, P.O., Sorooshian, A., Murphy, S.M. and Dalleska, N.F.: Effect of NOx level on secondary organic aerosol (SOA) formation from the photooxidation of terpenes. Atmospheric Chemistry and Physics, 7(19), 5159-5174, 2007.

Odum, J.R., Jungkamp, T.P.W., Griffin, R.J., Forstner, H.J.L., Flagan, R.C. and Seinfeld, J.H.: Aromatics, reformulated gasoline, and atmospheric organic aerosol formation. Environmental Science & Technology, 31(7), 1890-1897, 1997.